Available online at www.sciencedirect.com
ScienceDirect
Journal of Molecular Catalysis A: Chemical 277 (2007) 145–154
JOURNAL OF MOLECULAR CATALYSIS A: CHEMICAL
www.elsevier.com/locate/molcata

2-Propanol oxidation over gold supported catalysts coated ceramic foams prepared from stainless steel wastes

M.I. Domínguez [a,*], M. Sánchez [b], M.A. Centeno [a], M. Montes [b], J.A. Odriozola [a]

[a] *Instituto de Ciencia de Materiales de Sevilla, Centro Mixto CSIC-Universidad de Sevilla, Avda. Américo Vespucio 49, 41092 Sevilla, Spain*
[b] *Grupo de Ingeniería Química, Dpto. Química Aplicada, Fac. Ciencias Químicas de San Sebastián, UPV/EHU, Paseo Manuel de Lardizábal 3, 20018 San Sebastián, Spain*

Received 22 June 2007; received in revised form 19 July 2007; accepted 20 July 2007
Available online 26 July 2007

Abstract

Reticulated ceramic foams, prepared from steel making wastes using an earlier described multilayer replication method, have been used as support for preparing Au/Al_2O_3 and Au/CeO_2 catalytic devices, by depositing a coating of Al_2O_3 or CeO_2 and loading with gold by ion exchange. The obtained catalytic systems are active to the 2-propanol oxidation reaction, presenting the Au/CeO_2-coated monolith the best catalytic results because of the combination of the oxidation capability of gold atoms with the redox properties of the ceria phase.

Keywords: Gold catalysts; Wastes; 2-Propanol oxidation; Ceramic foams

1. Introduction

Slags and dusts are solid wastes generated during stainless steel production [1] and they need to be managed according to the current environmental laws. Slags are industrial wastes which have to be stored in authorised landfills. Dust is the solid waste recovered from fume filters and, because of its high content of toxic, leachable heavy metals such as Cr, Zn, Pb and Ni, has been qualified as hazardous waste by the European Waste Catalogue [2]. Nowadays, the destiny of this waste is its storage in security landfills or its use for metal recovering by means of a plasma process [3], implying both solutions a cost for the industry.

A previous paper [4] was devoted to these wastes valorisation by their use as raw material in the preparation of monolithic reticulated ceramic foams, by means of a multilayer replication method [5–7], to be used as catalytic systems for oxidation reactions.

Monoliths have reached in last decades an extended use in gas–solid catalysis, especially in the environmental field. Their properties make them useful devices for pollutants abatement in automobile exhaust or catalytic combustion [8].

Reticulated ceramic foams, thank to their structure of polyhedron shaped cells connected through windows, are highly porous materials. They are used in a great number of engineering applications, such as membranes, hot gas and diesel exhaust filters, refractory materials or biomaterials [5,9]. Nowadays, they are being applied as monolithic supports in catalysis because of its advantageous structure [10–13]. They share with honeycomb monolithic catalysts their low pressure drop and high geometric surface areas, what produce high external mass transfer rates. However, parallel channels in honey comb monoliths caused laminar flow, whereas foams have extensive pore tortuosity that produces turbulent flow, improving mixing and transport. These characteristics make these foams useful in processes where pressure drop, heat transfer and diffusion resistance are problems, like in highly endothermic or exothermic reactions [14–16].

Using the monolithic reticulated ceramic foams as supports, Au/Al_2O_3/support and Au/CeO_2/support catalytic devices have been prepared and their activity in the reaction of 2-propanol oxidation has been studied, as a probe molecule for oxygenated volatile organic compounds (VOCs).

The catalytic oxidation of VOCs is the election method for the abatement of VOC pollutants that have to be removed since their contribution to the production of ozone and photochemical smog [17]. Moreover, catalytic decomposition of 2-propanol is

* Corresponding author. Tel.: +34 954489543; fax: ++34 954460665.
E-mail address: mleal@icmse.csic.es (M.I. Domínguez).

1381-1169/$ – see front matter © 2007 Elsevier B.V. All rights reserved.
doi:10.1016/j.molcata.2007.07.038

frequently used as a test reaction to determine acid–base properties of metal oxides used as catalysts. The decomposition of 2-propanol occurs by two parallel reactions, dehydration to give propene, which is assumed to proceed at acidic sites, and dehydrogenation to give acetone, occurring at basic or redox sites. The hydrogenation of propene yields propane and its condensation benzene and, subsequently, cyclohexane. Acetone can undergo aldolic condensation to form diacetone alcohol (DAA) which can be dehydrated to produce mesityl oxide (MO). On strong acidic sites MO can react with acetone giving mesitylene. Finally, MO could hydrogenate to methyl isobutylketone (MIBK) [18–20].

Foams were washcoated using commercial colloidal alumina or ceria and calcined before gold loading by ion exchange. Gold was selected as active metal due to its high activity towards different reactions when present as nanoparticles on metal oxide supports [21,22]. The catalytic activity and stability of gold catalysts depend on the support, the size and distribution of gold particles and the properties of the contact surface gold support. The surface properties of the support strongly affect the final gold dispersion, and therefore, the catalytic performances of the solid [23,24].

Alumina and ceria were selected as supports due to their differences when interacting with gold particles. Alumina is an "inert support", being the activity of the resulting gold supported catalysts a strong function of the gold particle size. Nevertheless, CeO_2 is an "active support" because of its ability to provide reactive oxygen in the system what enhances the gold catalysts activity. In this second type of catalysts, the electronic properties of the support and the structure of the metal-support perimeter are more decisive than the size of the gold particles in the catalytic performances of the solid [25,26].

2. Experimental

2.1. Materials

Two solid wastes generated in stainless steel making, reduction slag and dust, have been employed as raw materials in this work. Reduction slag is produced in the AOD converter during the reduction step and has been preferred to other slags because of its higher silicium content, which diminishes the melting point and, consequently, permits a higher power saving in the preparation of the reticulated ceramic foams.

Dust is recovered from the fume filter system and has been selected by its high metal content that can improve the catalytic activity of the catalytic systems and because it is a hazardous waste which has to be inertised. Both wastes have been provided by ACERINOX S.A., a stainless steel factory placed in Cádiz (Spain).

Moreover, other additional materials have been used. Recycled silica, used as filler in chromatographic columns, and molten glass have been used to diminish the melting point of the waste mixtures. Portland cement has been employed due to its adhesive and setting properties. The chemical compositions of these materials were reported in an earlier paper [4]. Finally, commercial open-cell polyurethane foam of 15 pores per inch (ppi) supplied by Crestfoam and cut in cylinders of 15.8 mm diameter and 25 mm length was used as template.

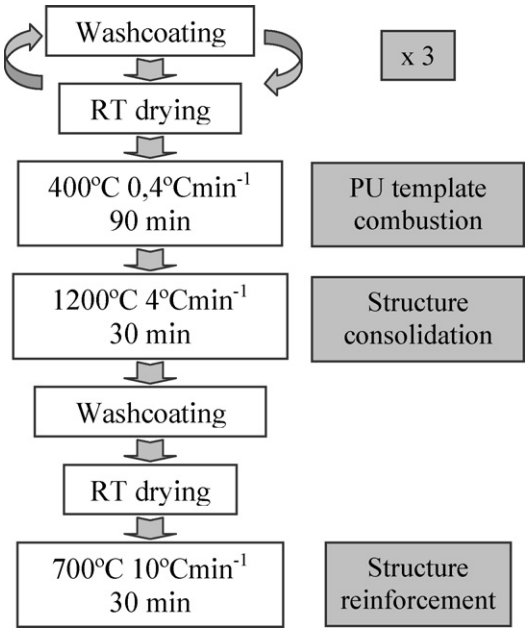

Fig. 1. Preparation process of the monolithic ceramic foams.

2.2. Preparation of catalytic systems

The details about the preparation method of the ceramic foam and its impregnation with gold have been reported elsewhere [4]. Ceramics foams have been prepared using a multilayer replication method which consists in the impregnation of the polymeric foam with several ceramic slurries containing steel making wastes and posterior thermal treatment to burn out the template and sinter the ceramic structure (Fig. 1). The obtained ceramic foams were wash-coated using commercial colloidal alumina and ceria (Nyacol) and calcined 2 h at 500 °C. Finally, gold was deposited on the foams by an ion exchange process, immersing the foam in a 9×10^{-4} M solution of $AuCl_4H{\cdot}3H_2O$ (Sigma, 99.9% pure) at pH 7 during 1 h. The resulted catalyst was dried overnight at 100 °C.

2.3. Characterisation techniques

Chemical composition of the obtained catalytic systems was analysed by X-ray fluorescence spectrometry (XRF), employing a Siemens SRS 3000 sequential spectrophotometer with a rhodium tube as source of radiation. XRF measurements were performed onto pressed pellets (sample including 10 wt% of wax).

X-ray diffraction (XRD) analysis was performed on a Siemens diffractometer D500. Diffraction patterns were recorded with Cu Kα radiation (40 mA, 40 kV) over a 2θ-range of 10–70° and a position-sensitive detector using a step size of 0.05° and a step time of 1 s.

The textural properties were studied by N_2 adsorption measurements at liquid nitrogen temperature. The experiences were

carried out in Micromeritics ASAP 2010 equipment, using a cell where the whole monolith was introduced. Before analysis, the samples were degassed for 2 h at 150 °C in vacuum.

Pressure drop has been measured using an electronic manometer (Digitron 2080, Sifam Instruments Limited).

The amount of gold deposited on the foams has been calculated by difference between the content of gold in the solution before and after the impregnation. Measurements were done with a Fisons ARL-3410 inductively coupled plasma atomic emission spectrometer.

2.4. Catalytic activity

The catalytic properties of the monoliths were followed by the ignition curves of 2-propanol. The catalytic tests were carried out in a conventional continuous flow U-shape glass reactor working at atmospheric pressure. The monolith (15.8 mm diameter and 25 mm length) is placed over a quartz wool and carborundum (Prolabo) bed (Fig. 2). This configuration is designed to premix and preheat the stream entering the reactor, obtaining a homogeneous temperature at the monolith inlet. A thermocouple in contact with the monolith assures the right measure of temperature. The reactor was surrounded by an electrical furnace equipped with a temperature programmer. Mass flow controllers (Bronkhorst) were used to prepare the feed mixture.

The light-off curves of 2-propanol oxidation (500 °C, 5 °C/min) were obtained with a mixture 21% O_2 in He saturated with 2-propanol at 0 °C and total flow rates of 14.3 and 253.2 ml/min. At established temperature, 2-propanol concentration is 12,000 ppm. Empty reactor (without monolith) shows no activity under such conditions. The catalysts were preactivated "in situ" during 1 h at 500 °C with a mixture of 21% O_2 in He at a flow of 30 ml/min and then stabilized at 100 °C before the introduction of the reaction mixture. After the 2-propanol adsorption equilibrium is reached, the light-off curve started.

The reaction was followed by mass spectrometry, using a Balzers Thermostar benchtop mass spectrometer controlled by the software Balzers Quadstar 422 with capabilities for quantitative analysis. m/z signals from 1 to 200 were recorded. As characteristic signals of the main compounds, m/z 45, 43, 41, 18 and 44 were assigned to 2-propanol and the main reaction products: acetone, propene, water and carbon dioxide, respectively. Side reactions will result in a wider set of products coming, mainly, from the aldolic condensation of acetone:

$$\text{Acetone} \rightarrow \text{DAA} \rightarrow \text{MO} \rightarrow \text{mesytilene} \rightarrow \ldots$$

The ascription of the m/z signals of the mass spectrum to any one of these products is not an easy task since most of the signals appear in more than one of these products. In order to assign one m/z signal unequivocally to these intermediates they were analysed by mass spectrometry and their characteristic signals elucidated. After this, the signal at $m/z = 55$ was associated to mesityl oxide (MO); $m/z = 69$ to 4-methyl-2-pentanol; $m/z = 100$ to methyl isobutylketone (MIBK) and $m/z = 105$ to mesitylene. Unfortunately, it was impossible to find a characteristic signal that can be unequivocally associated to DAA, a previous step in the production of MO that has been clearly identified within the reaction products. Therefore, the presence of MO has been taken as representative of the aldolic condensation of acetone taking place on our catalysts. It was necessary to correct the signals by subtracting from the characteristic signal of a product the contribution of another product, taking into account the intensity ratio between both products. Fig. 3 shows an example of this signal correction.

Fig. 2. Photograph of a prepared monolith into the U-shape glass reactor.

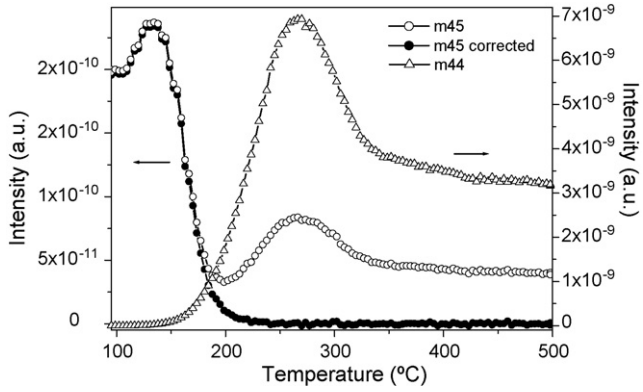

Fig. 3. Example of a m/z signal correction.

Table 1
Chemical composition of the prepared monolithic ceramic foams

Element (%weight)									
MgO	Al_2O_3	SiO_2	CaO	Cr_2O_3	MnO	Fe_2O_3	ZnO	MoO_3	NiO
1.42	1.12	17.46	49.60	5.35	3.28	13.12	5.10	1.99	1.56

Table 2
Determination of the gold content from ICP measurements on gold supported monolithic ceramics foams

Monolith	Au content (%weight)
Au/CeO_2-coated	0.06
Au/Al_2O_3-coated	0.015

From corrected results, light-off curves are obtained by plotting the *m/z* signal transformed in conversion versus temperature and the T_{50} value (temperature of the 50% conversion) is considered for practical applications as a measure of the activity.

3. Results and discussion

3.1. Catalyst characterization

The characterization results were reported in an earlier paper [4]. The most interesting data are reproduced here.

Table 1 presents the chemical composition of the obtained ceramic foam without catalytic layer. The amount of gold deposited on the coated monoliths is shown in Table 2. Gold content is four times higher in the CeO_2-coated monolith than in the Al_2O_3-coated one. This fact agrees with the reported preferential deposition of gold over ceria in CeO_2/Al_2O_3 systems, because of the more basic character of ceria compared to alumina [25,27].

The XRD diagrams of the obtained monoliths (not showed) reveal the presence of different high temperature silicates (larnite, akermanite, rankinite and pseudowollastonite), formed during the foam consolidation step at 1200 °C [28–30]. When the monolith is coated with ceria the characteristic peaks of cerianite are also observed. In the case of alumina-coated foams, this one is not detected by XRD because of its amorphous character. Gold has not been detected by XRD as result of its low percentage and/or crystalline domain size.

N_2 adsorption–desorption isotherms reveal the mesoporous character of the monoliths. BET surface areas of ceramic sponges without coating are lower than 1 $m^2\,g^{-1}$, increasing over 10 $m^2\,g^{-1}$ for Au/CeO_2 foams and above 20 $m^2\,g^{-1}$ for Au/Al_2O_3 ones (Table 3). If surface areas are recalculated only taking into account the weight of ceria or alumina and not the total weight of the monolith, the obtained values are between 75 and 100 m^2 per gram of CeO_2 for ceria monoliths and between 190 and 230 m^2 per gram of Al_2O_3 for alumina sponges. Moreover, not only BET surface area but pore diameter and pore volume are higher in Al_2O_3-coated monoliths than in CeO_2-coated ones, in good agreement with the textural properties of the CeO_2 and Al_2O_3 powders obtained after calcination at 500 °C of the commercial gels used in the foam impregnation (Table 3). It has to be noted that gold-impregnated monoliths present the highest surface areas. In this sense, Somorjai and co-workers found similar results in the incorporation of gold nanoparticles into silicate materials MCM-41 and MCM-48 [31] and based these observations on the expansion of the mesoporous structure of the support because of the introduction of gold nanoparticles inside the structure.

Washcoating does not produce a considerable increase in the pressure drop of the catalytic device. Pressure drop of non-coated monolith is similar to the obtained value for a ceramic monolith with 370 cpi (cells per inch); after coating its pressure drop is lower than the measured for a CSi foam of 20 ppi [32] (figure not showed).

3.2. Catalytic activity measures

3.2.1. Powder samples

With the aim of making easier the interpretation of the results obtained with monoliths, 2-propanol oxidation over pure Al_2O_3 and CeO_2 powder samples was also studied. Those samples were obtained by calcining at 500 °C the corresponding commercial colloidal solutions. Fig. 4 presents the evolution of the different species with temperature. As expected, propene is the only intermediate detected in the 2-propanol oxidation reaction over Al_2O_3, because of the acidic character of this support. On the other hand, acetone and MO are detected when CeO_2 is used, in agreement with its basic character and redox properties. Moreover, species C_xH_y, caused by the cracking of carbonaceous species adsorbed on the catalyst surface, are observed.

Table 3
Textural properties of the prepared ceramic foams and CeO_2 and Al_2O_3 powders obtained after calcinations at 500 °C of the commercial gels used in the foam impregnation process

	Non-coated	Al_2O_3-coated	Au/Al_2O_3-coated	CeO_2-coated	Au/CeO_2-coated	CeO_2-powder	Al_2O_3-powder
S_{BET} ($m^2\,g^{-1}$)	0.4	17.2	22.8	4.6	9.8	32.7	191.8
Pore volume ($cm^3\,g^{-1}$)	0.0005	0.0344	0.0492	0.0054	0.0128	0.0214	0.3749
Pore diameter (Å)	50.7	80.0	86.1	46.3	52.3	24.8	78.0

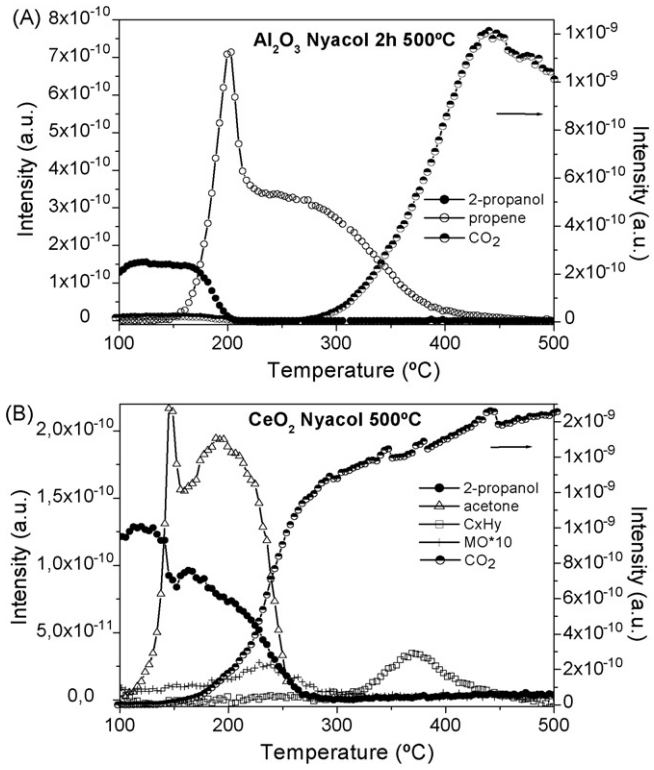

Fig. 4. Evolution of the different species with temperature during 2-propanol oxidation over Al_2O_3 and CeO_2 powders.

3.2.2. Monolithic systems

Fig. 5 presents the evolution of the intensities of propene, acetone, 2-propanol, MO and CO_2 *m/z* signals when 2-propanol oxidation is carried out at a flow rate of 14.3 ml min^{-1} over the prepared monoliths: Non-coated monolith (A), Al_2O_3-coated monolith (B), Au/Al_2O_3-coated monolith (C), CeO_2-coated monolith (D) and Au/CeO_2-coated monolith (E).

In alumina-coated monoliths (Fig. 5B and C) two facts are worth mentioning: (i) acetone is produced by dehydrogenation of 2-propanol; and (ii) the aldolic condensation of acetone results in species of higher molecular weight, as MO. Together with this, propene production through the dehydration of 2-propanol is observed. Finally, at higher temperatures, the total oxidation of 2-propanol to CO_2 takes place. The products distribution on both samples (Al_2O_3-coated monolith and Au/Al_2O_3-coated monolith) is similar, and only a little increase in the relative production of propene and MO is detected on Au/Al_2O_3-coated monolith. This observation suggests that gold hardly influences the catalytic properties of this system.

The formation of acetone is observed on the alumina-coated monoliths. The difference with the powdered catalyst has to be ascribed to the presence of metallic centres present in the monolith that comes from the used wastes. These metallic centres are responsible for the acetone production, the results obtained in the oxidation of 2-propanol using the non-coated monolith (Fig. 5A) were both propene, acetone and acetone condensation products (MO) are detected, allows ascribing the redox behaviour to the metallic ions present in the wastes. The intensity ratio between the *m/z* signals ascribed to propene and acetone is influenced by the presence of gold. For the gold-loaded monolith the acetone-to-propene ratio is smaller than in the case of the Al_2O_3-coated monolith, this, that cannot be related directly to the presence of gold, has to be associated to the modification of the ceramic foam due to the contact with the exchange solution used for depositing gold that results in leaching of the metallic cations from the ceramic foam, reducing the relative proportion of centres active in the dehydrogenation reaction that produces acetone.

As in the case of the alumina-coated monoliths, in the ceria-coated monoliths the influence of the ceramic foam is evident. In this case, the presence of propene can be easily seen in the ceria-coated monoliths while this product was completely absent in the case of the powdered ceria catalysts (Fig. 5D and E). As for the alumina-coated monoliths, this fact must be related to the monolith composition. Moreover, in these monoliths the intensity ratio of acetone-to-propene signals is markedly higher than in alumina-coated monoliths as should be expected if propene production is related to the acid–base centres of the ceramic foam. In the ceria-coated monoliths, as in the powdered solids, the ratio between acetone and propene yields is higher than in the case of alumina-coated monoliths. The high activity in the total oxidation combustion of the ceria catalysts is evident from the shift towards lower temperatures in the signal corresponding to CO_2 production. In the case of the ceria catalysts, the presence of gold eliminates the production of the "C_xH_y" species favouring the total combustion reaction. In this way, propene is hardly produced above 200 °C since the total oxidation reaction is favoured. The enhancement in the total oxidation reaction activity of the Au/CeO_2 prevents the formation of oxygenated products at temperatures above 250 °C increasing the selectivity towards CO_2 at these temperatures and avoiding the presence of products resulting from the aldolic condensation of acetone.

From the point of view of selectivity, the Au/CeO_2 coated monolith is the most interesting one. In the case of the alumina-coated monoliths, even considering that quantification is limited in these experiments, it can be concluded that dehydrogenation and dehydration reactions compete up to temperatures of ca. 300 °C. This results in the formation of acetone condensation products that produce a complex mixture in the reaction stream. The well known inert effect of the alumina support for gold catalysts causes the total oxidation reaction to occur at high temperatures and only well above 400 °C, it can be said that the combustion reaction results in 100% CO_2 yield both in the presence and absence of gold particles. On the contrary, for the case of ceria-coated monoliths the presence of supported gold particles allows distinguishing two reaction zones: (i) the low temperature zone (100–250 °C) where the intensity ratio between the acetone and propene signals is ca. 50 indicating a high selectivity towards the production of acetone with very low yields for the acetone condensation and dehydration products; and (ii) the high temperature region ($T > 250$ °C) where the Au/CeO_2-coated monoliths produces selectively CO_2.

From light-off curves obtained at a total flow rate of 14.3 ml min^{-1} (Fig. 6A and B), T_{50} values for 2-propanol disappearance (T_{50}P) and CO_2 production (T_{50}C) have been calculated and showed in Table 4. T_{50}P is, in all cases, lower than

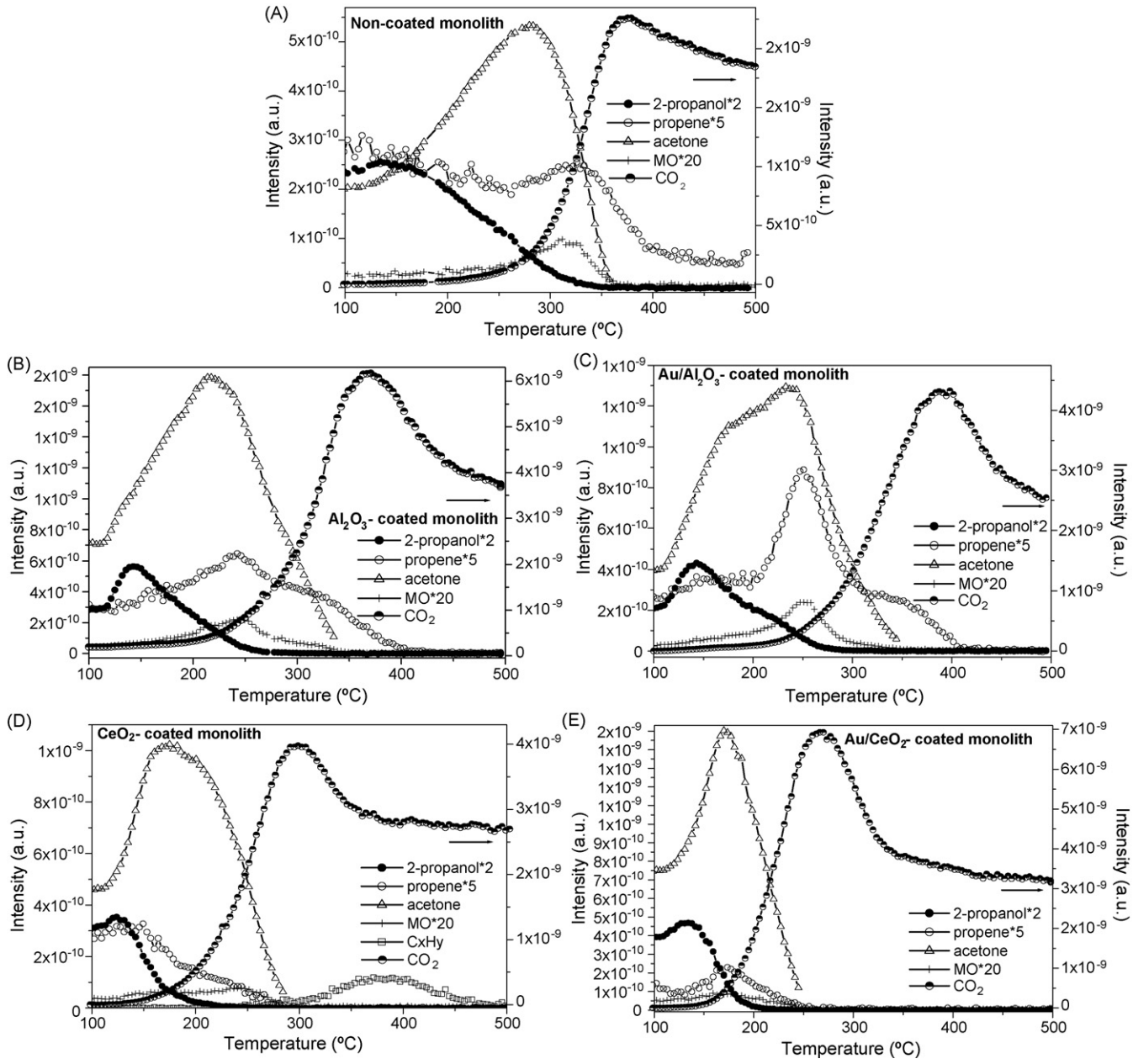

Fig. 5. Evolution of the different species with temperature during 2-propanol oxidation at 14.3 ml min^{-1} over non-coated monolith (A), Al_2O_3-coated monolith (B), Au/Al_2O_3-coated monolith (C), CeO_2-coated monolith (D) and Au/CeO_2-coated monolith (E).

T_{50}C, what is in agreement with the observed formation of intermediates. Moreover, if the non-coated monolith is excluded, a relationship between T_{50}P and S_{BET} is observed, in such a way that the higher is S_{BET}, the higher is T_{50}P. This may be related to an increased 2-propanol adsorption capacity on the catalyst surface, which is desorbed on increasing temperature.

Table 4
T_{50} values for 2-propanol disappearance and CO_2 formation

Monolith	T_{50}P (°C)	T_{50}C (°C)
Non-coated	253	321
Al_2O_3-coated	223	291
Au/Al_2O_3-coated	238	299
CeO_2-coated	158	233
Au/CeO_2-coated	169	197

Comparison of the T_{50}C for the studied monoliths reveals that CeO_2-coated monoliths present the best results, having the lowest T_{50}C the Au/CeO_2-coated monolith. Al_2O_3-coated monoliths present very similar T_{50}C values, which indicate a less important role of gold in 2-propanol oxidation respect to CO oxidation [4]. As expected by its low area and absence of gold, the non-coated monolith exhibits the highest values of T_{50}C and T_{50}P.

It is interesting to note that, at the beginning of the light-off curve (Fig. 6A), all monoliths present a 2-propanol desorption, which has been previously adsorbed on the saturation step. Higher is the S_{BET} of the monolith, higher is the extension of

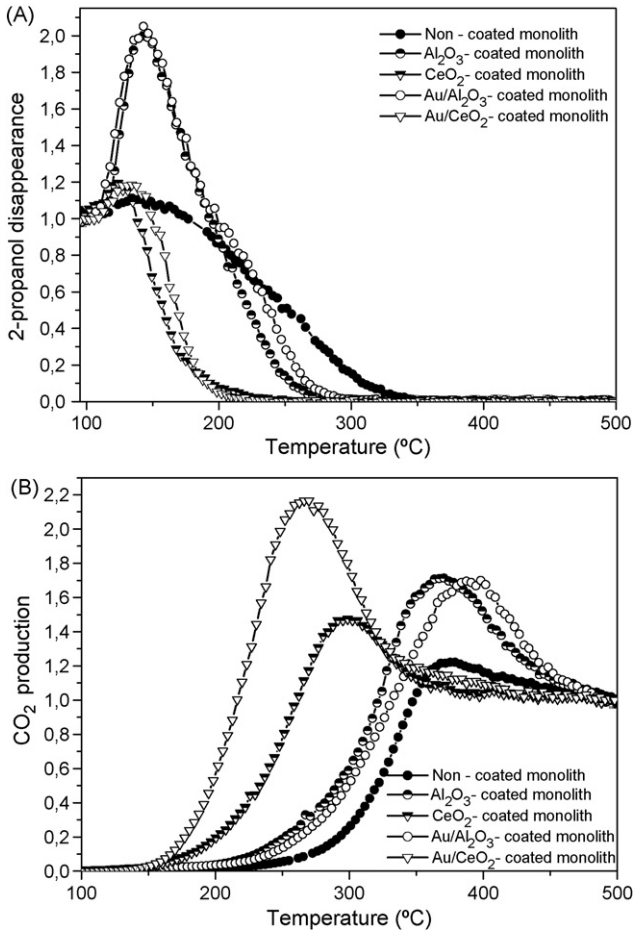

Fig. 6. Light-off curves obtained at a total flow rate of 14.3 ml min^{-1}: 2-propanol disappearance (A) and CO_2 production (B).

the observed desorption. This fact is illustrated in Fig. 7, where the area of the signal over 100% of conversion is plotted versus S_{BET} of the monoliths.

CO_2 signal has a similar behaviour, exceeding the 100% of conversion (Fig. 6B). This fact has been reported before [33] and has been associated to VOCs, intermediates and CO_2

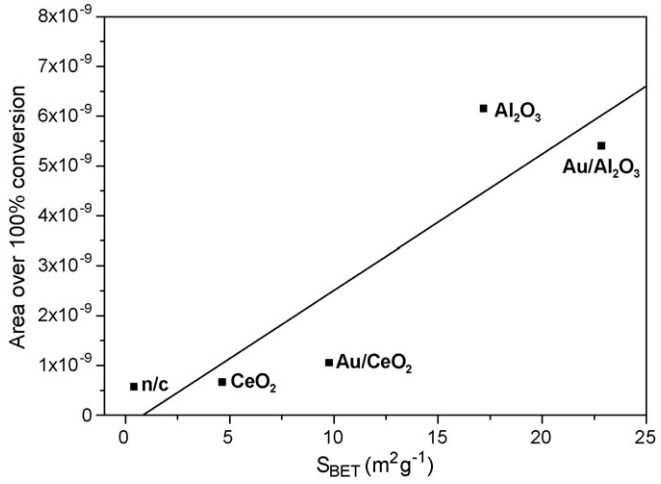

Fig. 7. Area of the 2-propanol signal over 100% of conversion vs. S_{BET} of the monoliths.

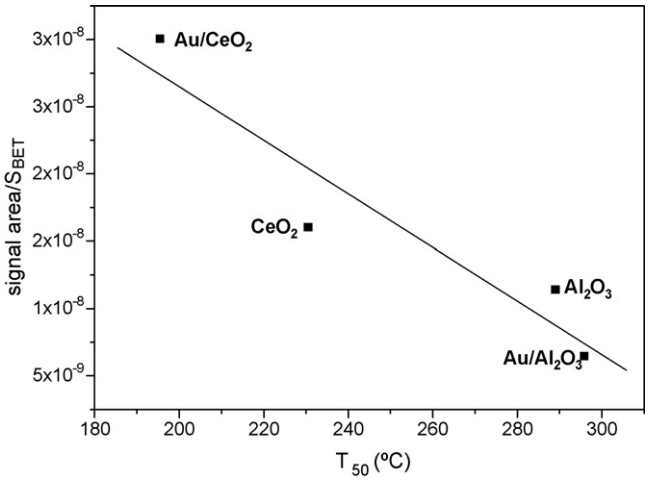

Fig. 8. Ratio CO_2 signal area over 100%/S_{BET} vs. T_{50}.

adsorption–desorption phenomena. When the activity of the active phase is high enough to start the oxidation at a sufficiently low temperature, close to that at which adsorption and desorption of the different species occurs, all these processes will be coupled provoking the observed phenomena. Moreover, the exothermic character of VOCs combustion will enhance these phenomena. In our case, they seem to be related with the surface area and the monolith activity. Fig. 8 shows this relationship by plotting the ratio of the signal area over 100% of production/S_{BET} versus T_{50}.

The influence of the total reactant flow on the catalytic activity has also been studied. The 2-propanol oxidation reactions have been studied at a total flow of 253.2 ml/min. As it should be expected, the intensity of the signals is smaller and maxima are displaced at higher temperatures (Fig. 9).

For the lower residence times the influence in the light-off curves of the adsorption–desorption phenomena is smaller. Fig. 10 shows the light-off curves for the Au/Al_2O_3-coated monolith as a function of the total flow, it can be seen that for the higher flow tested the adsorption–desorption phenomena are almost absent.

The CO_2 production curve obtained when Au/CeO_2-coated monolith is used could be deconvoluted in three processes (Fig. 11). The area under the curve representing each of them gives idea of its importance at the different tested flows.

At the highest flow tested, the only condensation product detected is MO that could be related to the shorter residence time. Conversion over 100% is only detected for CO_2 when the reaction is carried out on the Au/CeO_2 monolith; it has to be associated to the higher activity of this monolith (Fig. 12). In general, as stated above, shorter residence time broadens the signals of the different products, occurring their production in a wider temperature range, which influences negatively the selectivity. This is particularly important in the case of the Au/CeO_2-coated monolith where the intensity ratio of the acetone-to-propene signals decreases from ca. 50 to ca. 15 on going from 14.3 to 253.2 ml min^{-1}.

Finally, if T_{50} for the CO_2 production in the oxidation of CO [4] and in the oxidation of 2-propanol are compared (Table 5),

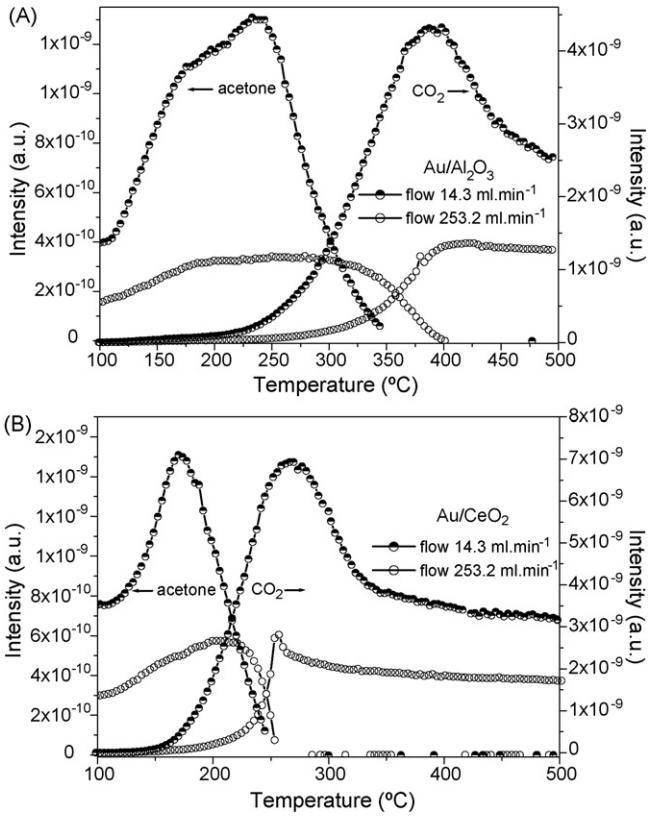

Fig. 9. Evolution of acetone and CO_2 signals with temperature during 2-propanol oxidation at studied flows (14.3 and 253.2 ml min^{-1}) over Au/Al_2O_3-coated monolith (A) and Au/CeO_2-coated monolith (B).

Table 5
T_{50} of CO_2 production in oxidation of CO [4] and in oxidation of 2-propanol

Monolith	CO_2 production T_{50} (°C) (CO oxidation)	CO_2 production T_{50} (°C) (2-propanol oxidation)
Non-coated	376	321
Al_2O_3-coated	373	291
Au/Al_2O_3-coated	216	299
CeO_2-coated	273	233
Au/CeO_2-coated	94	197

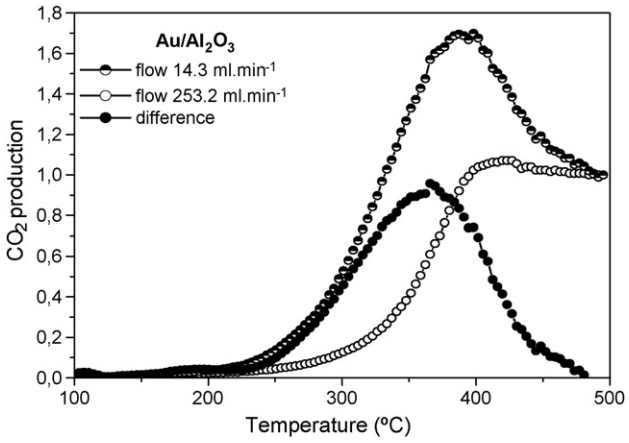

Fig. 10. CO_2 production curves at the studied flows and difference between both for Au/Al_2O_3-coated monolith.

Table 6
Difference between the T_{50} obtained using monoliths with and without gold for CO [4] and 2-propanol oxidation reactions

Support	ΔT_{50} CO	ΔT_{50} 2-propanol
Al_2O_3	157	−8
CeO_2	179	36

it is noticed that these temperatures are lower for 2-propanol oxidation on the alumina and ceria-coated monoliths. However, when these monoliths are gold-loaded the T_{50} values for the CO_2 production are lower in the CO oxidation reaction. This fact seems to point out to a more relevant role of gold in CO oxidation than in 2-propanol oxidation. This statement is clearly evidenced by calculating the difference between the T_{50} obtained using monoliths with and without gold for both oxidation reactions (Table 6), being these differences much more important in CO oxidation reaction. These results could be related with the accessibility of gold particles to the reactant molecules, being more accessible to a small molecule (CO) than to a more voluminous one (2-propanol) [27]. Moreover, these differences are higher in CeO_2-coated monoliths than in Al_2O_3-coated monoliths, because CeO_2 has the ability to suffer rapid reduction–oxidation cycles, increasing the capacity of the cata-

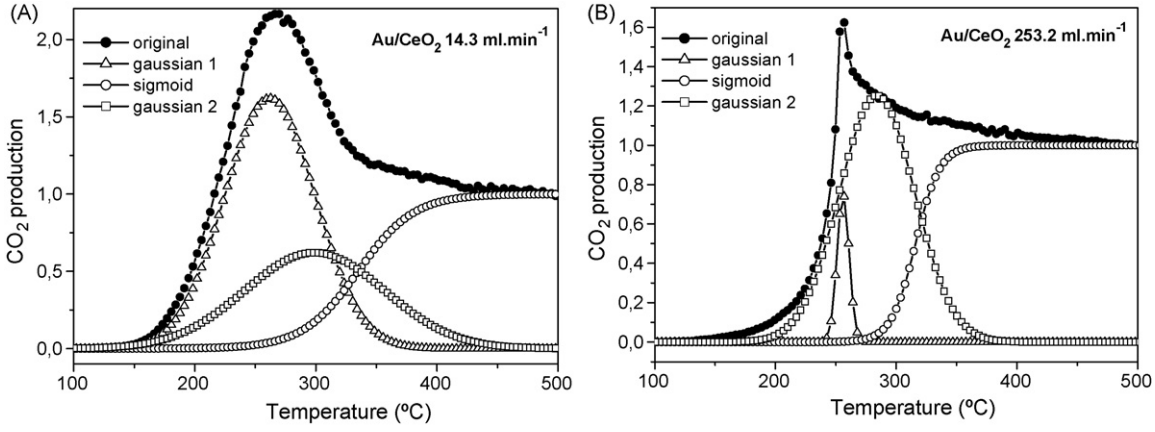

Fig. 11. CO_2 production curves deconvolution for Au/CeO_2-coated monolith at the studied flows: (A) 14.3 ml min^{-1} and (B) 253.2 ml min^{-1}.

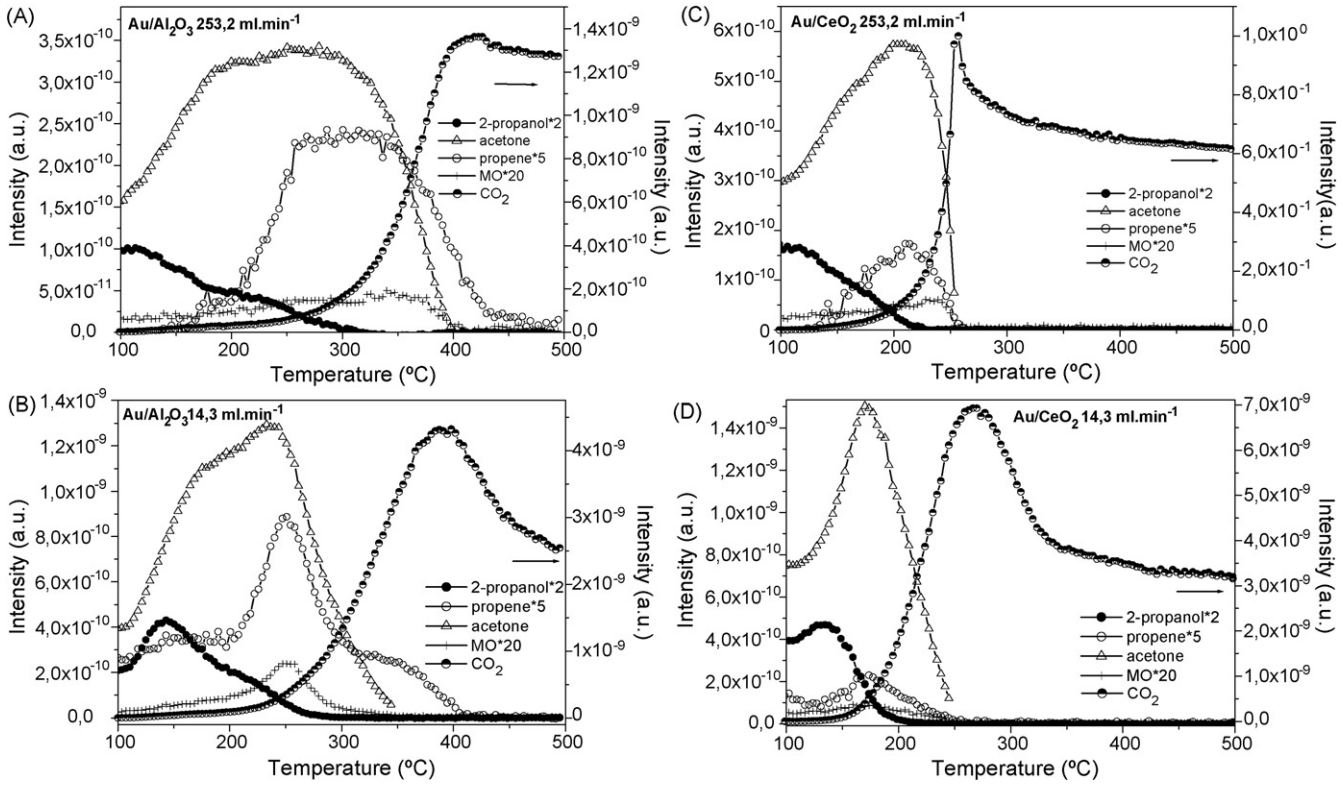

Fig. 12. Evolution of the different species with temperature during 2-propanol oxidation at the studied flows over Au/Al_2O_3-coated monolith: (A) 253.2 ml min^{-1}; (B) 14.3 ml min^{-1} and Au/CeO_2-coated monolith: (C) 253.2 ml min^{-1}; (D) 14.3 ml min^{-1}.

lyst for oxygen storage and improving in this way gold activity [25,27].

4. Conclusions

The ceramic foams prepared from steel making wastes by a replication method, using polyurethane sponge as template, can be used as catalyst support in the preparation of catalytic devices for 2-propanol oxidation. Non-coated, Al_2O_3-coated, CeO_2-coated, Au/Al_2O_3-coated and Au/CeO_2-coated monoliths have been tested in 2-propanol oxidation.

The obtained intermediates depend not only on the oxide used as support but on the monolith composition and the flow rate. In all cases, propene (intermediate produced on acidic sites), acetone and MO (intermediates produced on basic or redox sites) are detected, independently of the acid–base nature of the oxide, indicating the influence of monolithic composition in the obtained products. In Al_2O_3-coated monoliths and when the lowest flow is used, additional intermediates are produced (MIBK or mesitylene), what could be associated to a lower activity in comparison with CeO_2-coated monoliths.

As expected because of its inert character, alumina coating does not produce a noteworthy enhancement of the activity of the foam, while foams coated with ceria present a considerable improvement of their catalytic performances because of the redox properties of CeO_2. The best results are obtained for Au/CeO_2-coated monolith thanks to the combination of the enhanced oxygen storage capacity of the catalysts, due to the ceria redox properties, and the enhanced oxidation performances of the sample, due to the existence of surface metallic gold atoms.

The results show a more relevant role of gold in CO oxidation than in 2-propanol oxidation that could be related with the different accessibility of gold particles to the reactant molecules because of their different size.

Acknowledgements

Financial support for this work has been obtained from Spanish Ministerio de Ciencia y Tecnología, MCYT (MAT2006-12386-C05-01) and from Junta de Andalucía (Proyecto de Excelencia P06-TEP-01965). M.I.D. and M.S. thank the MCYT for the fellowship awarded. Finally, the authors thank ACERINOX S.A. and Crestfoam the supply of stainless steels solid wastes and polyurethane foams, respectively.

References

[1] L. Vadillo Fernández, Manual de reutilización de residuos de la industria minera, siderometalúrgica y termoeléctrica, Instituto Tecnológico Geominero de España, 1995.
[2] European Waste Catalogue, 2000/532/EC, amendments: 2001/118/EC, 2001/119/EC, 2001/573/EC.
[3] Scandust Company, www.scandust.se.
[4] M.I. Domínguez, M. Sánchez, M.A. Centeno, M. Montes, J.A. Odriozola, Appl. Catal. A 302 (2006) 96–103.
[5] E. Souza, C.B. Silveira, T. Fey, P. Greil, D. Hotza, A.P.N. Oliveira, Adv. Appl. Ceram. 104 (2005) 22–29.

[6] L. Montanaro, Y. Jorand, G. Fantozzi, A. Negro, J. Eur. Ceram. Soc. 82 (1998) 1339–1350.
[7] K. Schwartzwalder, A.V. Sommers: US patent 3,090,094, May 1963.
[8] P. Ávila, M. Montes, E.E. Miró, Chem. Eng. J. 109 (2005) 11–36.
[9] J. Luyten, I. Thijs, W. Wandermeulen, S. Mullens, B. Wallaeys, R. Mortelmans, Adv. Appl. Ceram. 104 (2005) 4–8.
[10] A. Wörner, C. Friedrich, R. Tamme, Appl. Catal. A 245 (2003) 1–14.
[11] B.A.A.L. van Setten, J. Bremmer, S.J. Jelles, M. Makkee, J.A. Moulijn, Catal. Today (1999) 613–621.
[12] D.W. Flick, M.C. Huff, Appl. Catal. A 187 (1999) 13–24.
[13] F. Scheffler, A. Zampieri, W. Schiwiegger, J. Zeschky, M. Scheffler, P. Greil, Adv. Appl. Ceram. 104 (2005) 43–48.
[14] F. Scheller, P. Claus, S. Schimpf, M. Lucas, M. Scheffler, in: P. Colombo, M. Schefller (Eds.), Cellular Ceramics: Structure, Manufacturing, Properties and Applications, Wiley-VCH, Weinheim, 2005.
[15] J.T. Richardson, Y. Peng, D. Remue, Appl. Catal. A 204 (2000) 19–32.
[16] J.T. Richardson, D. Remue, Y. Peng, Appl. Catal. A 250 (2003) 319–329.
[17] M.A. Centeno, M. Paulis, M. Montes, J.A. Odriozola, Appl. Catal. B 61 (2005) 177–183.
[18] D. Kulkarni, I.E. Wachs, Appl. Catal. A 237 (2002) 121–137.
[19] M.A. Hasan, M.I. Zaki, L. Pasupulety, J. Mol. Catal. A 178 (2002) 125–137.
[20] S.A. El-Molla, Appl. Catal. A 298 (2006) 103–108.
[21] G.C. Bond, D.T. Thompson, Catal. Rev. Sci. Eng. 41 (1999) 319–388.
[22] A.C. Gluhoi, S.D. Lin, B.E. Nieuwenhuys, Catal. Today 90 (2004) 175–181.
[23] M.A. Centeno, I. Carrizosa, J.A. Odriozola, Appl. Catal. A 246 (2003) 365–372.
[24] T. Tabakova, V. Idakiev, D. Andreeva, I. Mitov, Appl. Catal. A 202 (2000) 91–97.
[25] M.A. Centeno, C. Portales, I. Carrizosa, J.A. Odriozola, Catal. Lett. 102 (2005) 289–297.
[26] M.M. Schubert, S. Hackenberg, A.C. van Veen, M. Muhler, V. Plzak, R.J. Behm, J. Catal. 197 (2001) 113–122.
[27] M.A. Centeno, M. Paulis, M. Montes, J.A. Odriozola, Appl. Catal. A 234 (2002) 65–78.
[28] T.W. Cheng, J.P. Chun, C.C. Tzeng, Y.S. Chen, Waste Manage. 22 (2002) 485–490.
[29] J. Martínez-Frías, R. Benito, G. Wilson, A. Delgado, T. Boyd, K. Marti, J. Mater. Process. Technol. 147 (2004) 204–210.
[30] T. Toya, Y. Kameshima, A. Yasumori, K. Okada, J. Eur. Ceram. Soc. 24 (2004) 2367–2372.
[31] Z. Kónya, V.F. Puntes, I. Kiricsi, J. Zhu, J.W. Ager, M.K. Ko, H. Frei, P. Alivisatos, G.A. Somorjai, Chem. Mater. 15 (2003) 1242–1248.
[32] M. Sánchez, I. Legórburu, M.A. Centeno, J.A. Odriozola, M. Montes, Proc. XIX Simposio Iberoamericano de Catálisis (2004) 2496–2503.
[33] M. Paulis, L.M. Gandía, A. Gil, J. Sambeth, J.A. Odriozola, M. Montes, Appl. Catal. B 26 (2000) 37–46.